

## Clast morphology of the Siwalik conglomerates from the Dhan Khola Formation, Surai Khola area, Mid-Western Nepal

Naresh Kazi Tamrakar

Central Department of Geology, Tribhuvan University, Kirtipur, Kathmandu, Nepal

### ABSTRACT

Clast morphology of the Siwalik conglomerates from the Dhan Khola Formation was studied at 19 horizons. The clasts were measured to calculate morphological indices such as axial ratios,  $c/a$  and  $(a-b)/(a-c)$ , maximum projection sphericity ( $\psi_p$ ), coefficient of flatness (CF), and roundness ( $\rho$ ) separately for quartzite clasts (with two size-grades) and other clasts. The shape indices were plotted in shape diagrams and statistical tests were used to compare the shape indices of the above clasts with the index limits proposed in earlier studies.

Based on clast type, four units are proposed for the Dhan Khola Formation. The formation is sub-divided into the volcanic clast-dominated, dolomite clast-dominated, quartzite clast-dominated, and terrigenous clast-dominated units, respectively from bottom to top. The latter unit contains many clasts derived from the Siwaliks. The quartzite clasts are more compact than other ones with significant differences in their axial ratios. The quartzite clasts show textural abnormalities and their  $\rho$  values decrease in the upper part of the formation suggesting high rate of sediment supply and nearness of complex source. The quartzite clasts with smaller ( $>4\phi$ ) size-grade are better sphered. They plot clearly in the fluvial field of the  $\psi_p$  versus CF diagram. In 60 % of the quartzite clasts, means of  $\psi_p$  and CF exceed significantly the lower index limits showing that they were shaped in fluvial environment. However, the samples giving insignificant results could have also formed under the same conditions but with  $\psi_p$  and CF values lower than index limits proposed earlier.

### INTRODUCTION

The Siwalik Group is recognised as a thick fluvial deposit consisting of mudstone and fine sandstone in the lower part and conglomerate in the upper part. This overall coarsening-upward sequence has been interpreted as a consequence of upliftment and unroofing of the rising Himalayas in the north (Tokuoka et al. 1986; Tokuoka 1992). Conglomerate sequences in the Siwaliks of West Nepal have been interpreted as braided to mid-fan deposits (Tokuoka 1992). Corvinus (1992) and Dhital et al. (1995) have studied stratigraphy of the group in the Surai Khola area. The Dhan Khola Formation is the youngest sequence having a total thickness of 1080 m of which conglomerates attain a cumulative thickness of 760 m (Dhital et al. 1995). The formation has been described to contain cobble-pebble polymictic conglomerates of indurate nature in the lower part and boulder-cobble conglomerate in the upper part (Tamrakar 1993). The palaeomagnetic age assigned to these conglomerate-rich sequences is younger than 2.3 Ma (Appel et al. 1991).

Study on clast morphology of conglomerate is considered a tool in understanding conditions under which clasts were deposited (Pettijohn 1984). Shape indices as maximum projection sphericity ( $\psi_p$ ), axial ratios, coefficient of flatness (CF) and oblate-prolate indices are interpreted as useful environmental indicators and are widely used by Dobkin and Folk (1970), Stratten (1974), and Barrett (1980). Howard

(1992) used the shape indices to discriminate between the fluvial, beach, and fan conglomerates. Els (1988) used the indices to compare with those determined as limit by Stratten (1974). Both of them have interpreted limited usefulness of oblate-prolate index as a palaeoenvironmental indicator. They have found the plot of sphericity versus coefficient of flatness quite useful.

The Dhan Khola Formation comprising numerous conglomerate beds was selected for the study of clast morphology. Samples were obtained from 19 different conglomerate horizons in the vertical sequence. Shape indices such as  $\psi_p$ , axial ratios (Sneed and Folk 1958), CF (Luttig 1962), and roundness (Folk 1955) were calculated for quartzite and other clasts as well as for two size-grades of quartzite clasts to see if there exists any difference in indices between clasts of different composition and/or clasts of two size-grades of similar composition. Roundness values are evaluated to see whether there is textural inversion (Folk 1980). Means of sphericity and coefficient of flatness of quartzite clasts and other clasts are compared with index limits used in earlier studies. Statistical tests were used to understand the significance of the results. The shape diagram of Sneed and Folk (1958) was used to interpret axial ratios. It was contoured for representation of shapes of clasts. Besides, the clasts were counted from each conglomerate bed to reveal their compositional variation trend in the vertical sequence.



## GEOLOGICAL SETTINGS

The Siwaliks of Mid-Western Nepal can be recognised as low hills (<1500 m high) bordered in the north by the Main Boundary Thrust (MBT) and in the south by the Main Frontal Thrust (MFT). The study area lies in the southern part of the Siwaliks, which constitute a monoclinical sequence in between the Rangsing Thrust (RT) and the MFT, respectively in the north and south. The monocline is made up of a continuous northward-younging succession with dips essentially due N (Fig. 1).

### Lithostratigraphy

The Siwalik Group of the study area is composed of thick fluvial sequence (>5 km) of mudstones, siltstones, marls, sandstones, and conglomerates. It is divided into the Bankas, Chor Khola, Surai Khola, Dobata, and the Dhan Khola Formations (Dhital et al. 1995) in an ascending order (Fig. 1). Further, Dhital et al. (1995) sub-divided the Chor Khola Formation into the Jungli Khola Member and the Shivgarhi Member from older to younger, on the basis of lithological characteristics of mudstones and sandstones. The palaeomagnetic age assigned by Appel et al. (1991) varies between 13 Ma for the oldest unit, the Bankas Formation, and < 2.3 Ma for the youngest unit, the Dhan Khola Formation.

The Bankas Formation is characterised by fine- to medium-grained sandstones, bioturbated and variegated siltstones, mudstones, and calcretes. The Chor Khola Formation is distinguished by thick, coarse- to medium-grained sandstones (Dhital et al. 1995). Variegated mudstones occur in the Jungli Khola Member, whereas green-grey mudstones predominate in the Shivgarhi Member. Besides cyclic deposits of very thick-bedded, coarse- to very coarse-grained 'salt and pepper' sandstones, there are also interbedded siltstones and mudstones. Marl beds (limestones of Corvinus 1992) occurring in the uppermost part of the Chor Khola Formation, where they are overlain by 'salt and pepper' sandstones, show the boundary (Corvinus 1992) between the Chor Khola Formation and the Surai Khola Formation.

The Surai Khola Formation is easily distinguished because of the multi-storeyed nature (Corvinus 1992) of coarse-grained lithic sandstones (Tamrakar 1998) with various sedimentary structures. The sandstone sequences are followed by the mudstone-predominating unit called the Dobata Formation, which contains pebbly to coarse-grained sandstones with sand balls interbedded with light yellow, grey, green-grey, and brown mudstones.

The Dhan Khola Formation crops out as the uppermost part of the Siwalik Group and distributes in the monoclinical sequence south of the RT. Along the East-West Highway, the sequence is better exposed and is more-or-less continuous. The formation comprises cobble-pebble conglomerates, mudstones and sandstones in the lower part and loose cobble-, to boulder-conglomerates interbedded with loose yellow mudstones in the upper part (Corvinus

1992; Dhital et al. 1995; Tamrakar 1998). The formation is 1080 m thick where cumulative thicknesses of conglomerates, mudstones and sandstones are 760 m (70%), 285 m (27%), and 35 m (3%), respectively (Dhital et al. 1995).

## METHOD

Random sampling (Howard 1993) of conglomerates was carried out along the highway and in the streams near the Dhan Khola bridge and the Rangsing Khola throughout the stratigraphic sequence. Nineteen sampling sites were selected in a vertical succession. An area method of counting (Howard 1993) was adopted for sampling. For this purpose, 1 m<sup>2</sup> of area was selected perpendicular to bedding surfaces and about 100 clasts (greater than 1 cm in size) were counted. The amount of matrix and cement was estimated on visual basis on that area.

For the study of morphology, 70 to 120 clasts were picked out from the 1 m<sup>2</sup> area (which was enlarged whenever necessary) avoiding breakage and were categorised into quartzite and other clasts. For the determination of roundness, three-dimensional images of clasts were compared with the modified Powers' image chart (Lindholm 1987). The chart was enlarged for convenience and each clast was assigned to the roundness class of Powers (Lindholm 1987). The number of frequencies obtained was used to calculate mean roundness value,  $\rho$ . The long (a), intermediate (b), and short (c) axes of each clast were measured and their ratios,  $c/a$  and  $(a-b)/(a-c)$ , and  $\psi_p$  of Sneed and Folk (1958), and CF of Luttig (1962) were calculated. Means and standard deviations of shape indices were calculated for quartzite and other clasts and for different size grades of quartzite clasts. Axial ratios are represented using the shape diagrams (Sneed and Folk 1958) and are contoured following Perez (1987).

Values obtained for shape indices were tested to fit a normal distribution. For this, each observation in sample was transferred to z-score value, and was categorised into four classes of equal region in terms of z-scores, as  $-\infty$  to  $-0.67$ ,  $0$  to  $0.67$ , and  $0.67$  to  $+\infty$ . In the standard normal curve, each class should contain 25% of the values. Therefore, the frequencies obtained in each class after assigning z-scored values are taken as observed frequencies to calculate chi-squared values. Chi-squared tests (Kooosis and Coladarci 1985) were used applying the following relationship:

$$\chi^2 = S(O_f - E_f)^2 / E_f$$

where,  $O_f$  and  $E_f$  are respectively observed frequency and expected (in this case 25%) frequency in each of four classes.

Other statistical approaches used were t-test and z-test. The t-tests was used to see any significant differences between shape indices of quartzite and other clasts, using the following expressions:

$$t = (x_1 - x_2) / \sqrt{(S^2/n_1) + (S^2/n_2)}$$



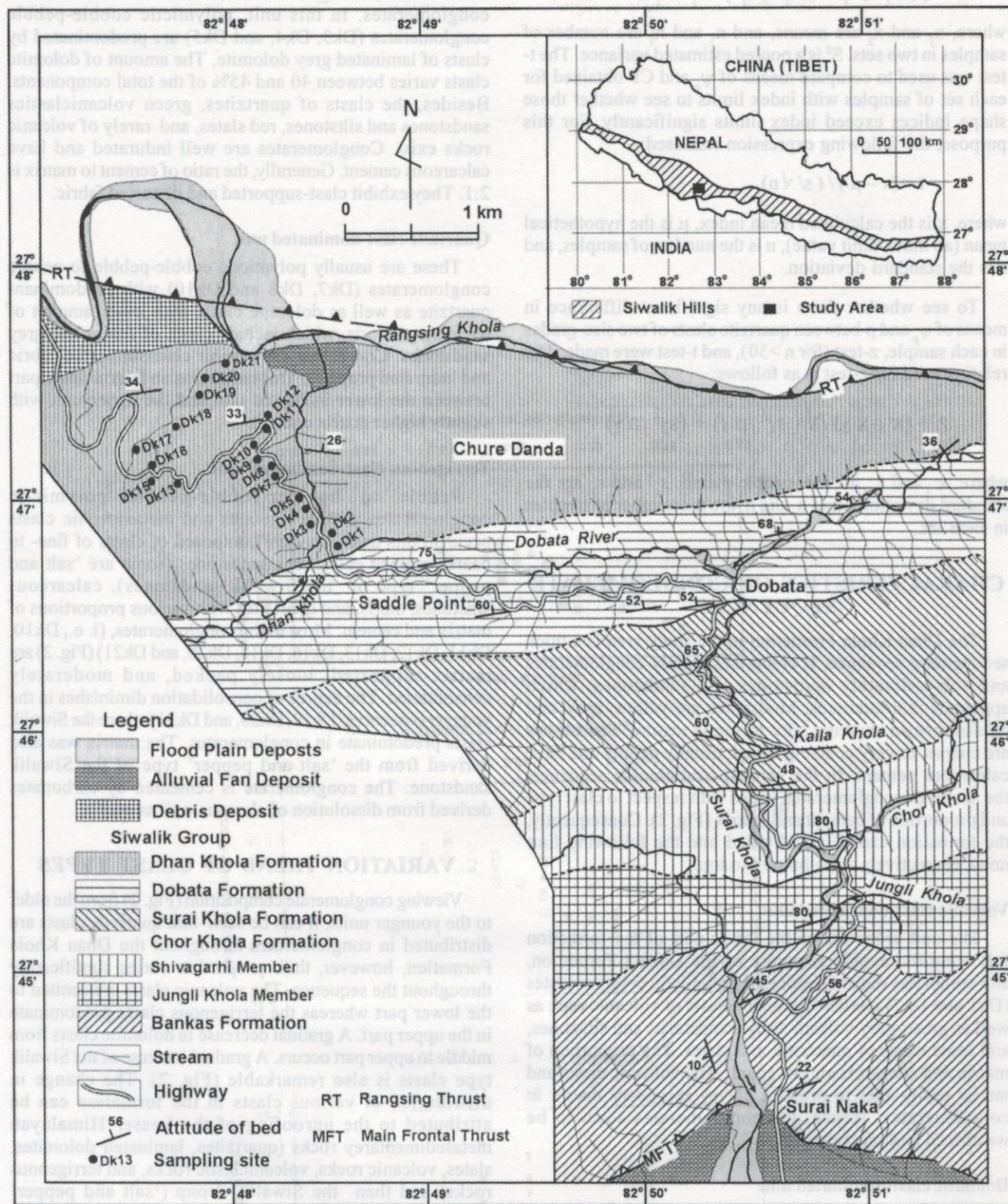


Fig. 1: Geological map (after Dhital et al. 1995) showing locations of conglomerate sampling sites



$$S^2 = \{ (n_1 - 1) s_1^2 + (n_2 - 1) s_2^2 \} / n_1 + n_2 - 2$$

where,  $x_1$  and  $x_2$  are means, and  $n_1$  and  $n_2$  are number of samples in two sets.  $S^2$  is a pooled estimated variance. The t-test was used to compare means of  $\psi_p$  and CF obtained for each set of samples with index limits to see whether those shape indices exceed index limits significantly. For this purpose, the following expression was used:

$$t = (x - \mu) / (s / \sqrt{n})$$

where,  $x$  is the calculated mean index,  $\mu$  is the hypothetical mean (an index limit value),  $n$  is the number of samples, and  $s$  is the standard deviation.

To see whether there is any significant difference in means of  $\psi_p$  and  $\rho$  between quartzite clasts of two size-grades in each sample, z-test (for  $n > 30$ ), and t-test were made. The relation used for z-test is as follows:

$$z = (x_1 - x_2) / \sqrt{(s_1^2 / n_1) + (s_2^2 / n_2)}$$

where,  $x_1$  and  $x_2$  are the sample means,  $s_1$  and  $s_2$  are the standard deviations, and  $n_1$  and  $n_2$  are the number of samples in each set.

## CHARACTERISTICS OF CONGLOMERATE SEQUENCES

The Dhan Khola Formation in the study area is a thick sedimentary sequence. It comprises mainly conglomerates and sub-ordinately mudstones and sandstones, which appear as thin interbeds. Mudstones are yellow, grey, and reddish brown showing silty to sandy texture. Sandstones are coarse- to very coarse-grained, usually pebbly and have calcareous cement. In the vertical stratigraphic sequence, the nature of conglomerates varies with respect to clast type and proportion of cement and matrix (Fig. 2). Consequently, the formation can be sub-divided into the following four units, respectively from bottom to top.

### Volcanic clast-dominated unit

The unit crops out in the lower part of the formation following the muddy sequence of the Dobata Formation, and comprises matrix-supported polymictic conglomerates (Dk1 and Dk2) containing many clasts of volcanic rock as well as green-grey volcanoclastic sandstones and siltstones, and some clasts of quartzites and slates. The proportion of matrix and cement is almost equal. The volcanic clasts and matrix easily alter to produce clayey secondary matrix in conglomerates. Hence, the conglomerates seem to be weathered and incompetent.

### Dolomite clast-dominated unit

This rock was interpreted as hard cemented conglomerates with abundant limestone cobbles by Corvinus (1992). This unit transitionally follows the former one and forms more-or-less a prominent ridge called the

Chure Danda, owing to calcareous and indurated nature of conglomerates. In this unit, polymictic cobble-pebble conglomerates (Dk3, Dk4, and Dk5) are predominated by clasts of laminated grey dolomite. The amount of dolomite clasts varies between 40 and 45% of the total components. Besides, the clasts of quartzites, green volcanoclastic sandstones and siltstones, red slates, and rarely of volcanic rocks exist. Conglomerates are well indurated and have calcareous cement. Generally, the ratio of cement to matrix is 2:1. They exhibit clast-supported and ill-sorted fabric.

### Quartzite clast-dominated unit

These are usually polymictic cobble-pebble to pebble conglomerates (Dk7, Dk8 and Dk10) with predominant quartzite as well as dolomite clasts with lesser amount of terrigenous clasts, which include clasts of shales and grey sandstones. Conglomerates exhibit clast-supported fabric and indurated property. This unit forms an intermediate part between the lower indurated unit and the upper unit with slightly higher matrix content.

### Terrigenous clast-dominated unit

Pebble to boulder-cobble-pebble polymictic conglomerates with terrigenous and metamorphic clasts occur in this unit. They are composed of clasts of fine- to coarse-grained calcareous sandstones (some are 'salt and pepper' type of the Siwalik sandstones), calcareous siltstones, marls, and quartzites with various proportions of matrix and cement. Most of the conglomerates, (i. e., Dk10, Dk11, Dk12, Dk13, Dk16, Dk18, Dk20, and Dk21) (Fig. 2) are matrix-supported, loosely packed, and moderately consolidated. The degree of consolidation diminishes in the younger sequences (Dk19, Dk20, and Dk21) where the Siwalik clasts predominate in conglomerates. The matrix was also derived from the 'salt and pepper' type of the Siwalik sandstone. The conglomerate is cemented by carbonates derived from dissolution of clasts as well as matrix.

## VARIATION TREND OF CLAST TYPES

Viewing conglomerate composition (Fig. 2) from the older to the younger units, it can be seen that quartzite clasts are distributed in conglomerates throughout the Dhan Khola Formation, however, their proportion varies significantly throughout the sequence. The volcanic clasts are limited to the lower part whereas the terrigenous clasts predominate in the upper part. A gradual decrease in dolomite clasts from middle to upper part occurs. A gradual increase of the Siwalik type clasts is also remarkable (Fig. 2). The change in distribution of various clasts in the formation can be attributed to the unroofing of the Lesser Himalayan metasedimentary rocks (quartzites, laminated dolomites, slates, volcanic rocks, volcanoclastic rocks, and terrigenous rocks) and then the Siwalik Group ('salt and pepper' sandstone, siltstone, calcareous shale, and marl). At that time, there was also a change in the rate of sediment supply. Appearance of clasts of the Siwalik type is attributed to initiation of unroofing of the Siwalik Group (Tokuoka 1992),



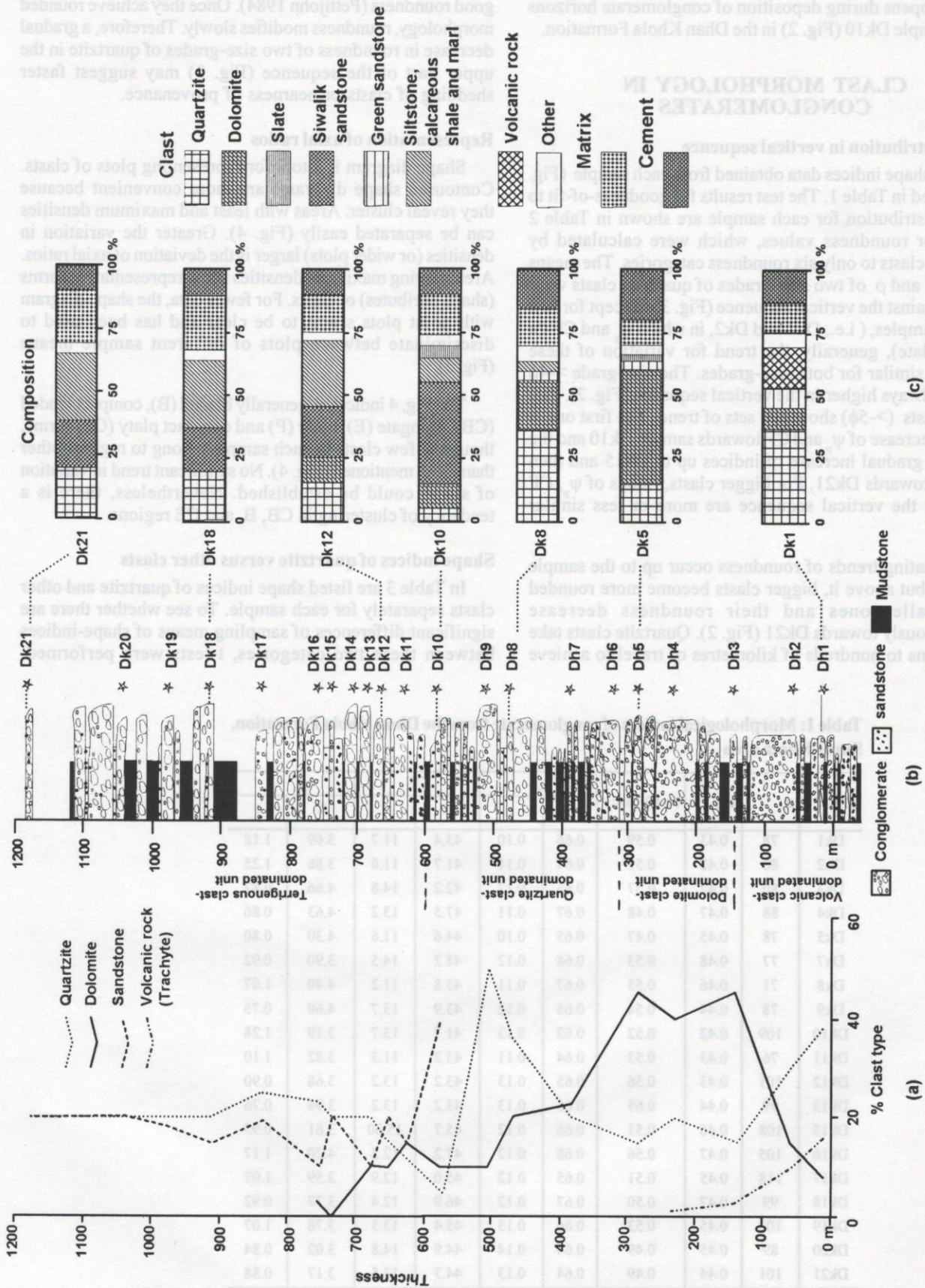


Fig. 2: Diagram showing (a) changes in dominant clast-type in vertical sequence, (b) columnar section of the Dhan Khola Formation (after Dhital et al. 1995) revealing sample horizons, and (c) composition of conglomerates. Notice that from DK10 upwards, the Siwalik increase significantly.



which happens during deposition of conglomerate horizons above sample Dk10 (Fig. 2) in the Dhan Khola Formation.

### CLAST MORPHOLOGY IN CONGLOMERATES

#### Shape distribution in vertical sequence

Clast shape indices data obtained from each sample (Fig. 1) are listed in Table 1. The test results for goodness-of-fit to normal distribution for each sample are shown in Table 2 except for roundness values, which were calculated by assigning clasts to only six roundness categories. The means of  $\psi_p$ , CF, and  $\rho$  of two size-grades of quartzite clasts were plotted against the vertical sequence (Fig. 3). Except for two plots of samples, (i.e., Dk1 and Dk2, in which  $\psi_p$  and CF do not correlate), generally, the trend for variation of these indices is similar for both size-grades. The size-grade  $>-4\phi$  remains always higher in the vertical sequence (Fig. 2). The bigger clasts ( $>-5\phi$ ) show two sets of trend. The first one is gradual decrease of  $\psi_p$  and CF towards sample Dk10 and the second is gradual increase of indices up to Dk15 and then decrease towards Dk21. For bigger clasts, trends of  $\psi_p$ , CF and  $\rho$  in the vertical sequence are more or less similar (Fig. 3).

Fluctuating trends of roundness occur up to the sample of Dk15, but above it, bigger clasts become more rounded than smaller ones and their roundness decrease simultaneously towards Dk21 (Fig. 2). Quartzite clasts take several tens to hundreds of kilometres of travel to achieve

good roundness (Pettijohn 1984). Once they achieve rounded morphology, roundness modifies slowly. Therefore, a gradual decrease in roundness of two size-grades of quartzite in the upper part of the sequence (Fig. 3) may suggest faster shedding of clasts or nearness of provenance.

#### Representation of axial ratios

Shape diagram is a tool for representing plots of clasts. Contoured shape diagrams are more convenient because they reveal cluster. Areas with least and maximum densities can be separated easily (Fig. 4). Greater the variation in densities (or wider plots) larger is the deviation of axial ratios. Areas having maximum densities show representative forms (shape attributes) of clasts. For fewer data, the shape diagram with point plots seems to be clear and has been used to discriminate between plots of different sample means (Fig. 5).

The Fig. 4 indicates, generally bladed (B), compact bladed (CB), elongate (E), platy (P) and compact platy (CP) forms, though a few clasts in each sample belong to regions other than those mentioned (Fig. 4). No significant trend in variation of shape could be established. Nevertheless, there is a tendency of clustering in CB, B, and CE regions.

#### Shape indices of quartzite versus other clasts

In Table 3 are listed shape indices of quartzite and other clasts separately for each sample. To see whether there are significant differences of sampling means of shape-indices between these two categories, t-tests were performed.

**Table 1: Morphological indices of conglomerate from the Dhan Khola Formation, Surai Khola area**

Bed	n	c/a	(a-b)/(a-c)	$\psi_p$		CF		$\rho$	
				x	s	x	s	x	s
Dk1	78	0.43	0.59	0.66	0.10	43.4	11.7	3.69	1.18
Dk2	80	0.42	0.55	0.64	0.11	41.7	11.6	3.86	1.25
Dk3	80	0.42	0.57	0.65	0.17	42.2	14.8	4.66	0.82
Dk4	88	0.47	0.48	0.67	0.11	47.5	13.2	4.63	0.86
Dk5	78	0.45	0.47	0.65	0.10	44.6	11.6	4.30	0.80
Dk7	77	0.48	0.53	0.68	0.12	48.2	14.5	3.90	0.92
Dk8	71	0.46	0.55	0.67	0.11	45.8	11.2	4.40	1.07
Dk9	78	0.44	0.54	0.65	0.12	43.9	13.7	4.60	0.75
Dk10	109	0.42	0.52	0.62	0.13	41.7	13.7	3.19	1.28
Dk11	76	0.43	0.53	0.64	0.11	43.2	11.3	3.82	1.10
Dk12	101	0.43	0.56	0.65	0.13	43.2	13.2	3.68	0.90
Dk13	99	0.44	0.65	0.65	0.13	43.2	13.2	3.94	0.76
Dk15	108	0.46	0.51	0.66	0.12	45.7	15.30	3.61	0.95
Dk16	105	0.47	0.56	0.68	0.12	47.2	12.8	4.20	1.17
Dk17	118	0.45	0.51	0.65	0.12	45.0	12.9	3.59	1.07
Dk18	99	0.47	0.50	0.67	0.12	46.9	12.4	3.77	0.92
Dk19	103	0.45	0.53	0.66	0.13	45.4	13.5	3.78	1.07
Dk20	89	0.45	0.49	0.64	0.14	44.9	14.8	3.02	0.84
Dk21	101	0.44	0.49	0.64	0.13	44.3	13.5	3.17	0.88



Table 2: Chi-squared values for goodness-of-fit test

Bed	n	c/a	(a-b)/(a-c)	$\psi_p$	CF
Dk1	78	1.38	0.87	2.10	2.72
Dk2	80	0.70	4.00	0.30	1.70
Dk3	80	1.12	1.32	1.22	1.12
Dk4	88	2.27	2.27	5.73	2.09
Dk5	78	1.15	0.34	4.70	2.57
Dk7	77	4.92	1.70	2.01	3.88
Dk8	71	0.72	3.42	0.83	1.17
Dk9	78	4.00	0.10	0.50	2.60
Dk10	109	3.84	1.35	2.23	2.96
Dk11	76	0.10	0.11	2.00	0.11
Dk12	101	1.46	0.54	2.85	1.46
Dk13	99	3.96	0.20	5.10	2.82
Dk15	108	2.00	0.30	1.41	1.70
Dk16	105	1.27	3.14	0.18	1.66
Dk17	118	0.52	1.40	0.52	0.52
Dk18	99	3.24	6.04	3.51	3.24
Dk19	103	1.19	5.00	1.35	2.67
Dk20	89	2.01	4.26	0.66	2.91
Dk21	101	0.74	2.80	2.09	1.06

Critical  $\chi^2 = 7.81$  (df = 3 and P = 0.05)

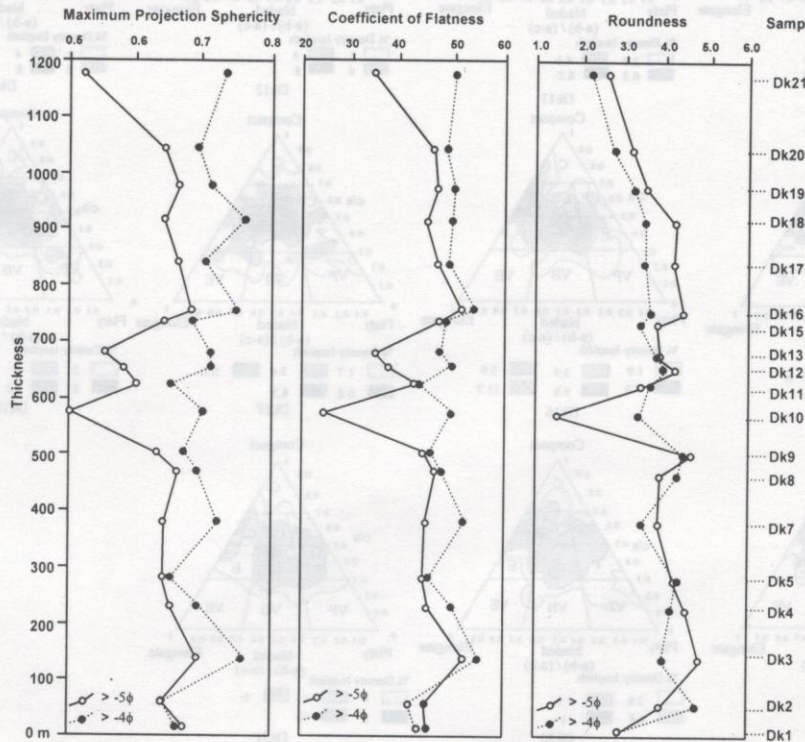


Fig. 3: Distribution of shape indices of different size grades of quartzite clasts in the vertical sequence



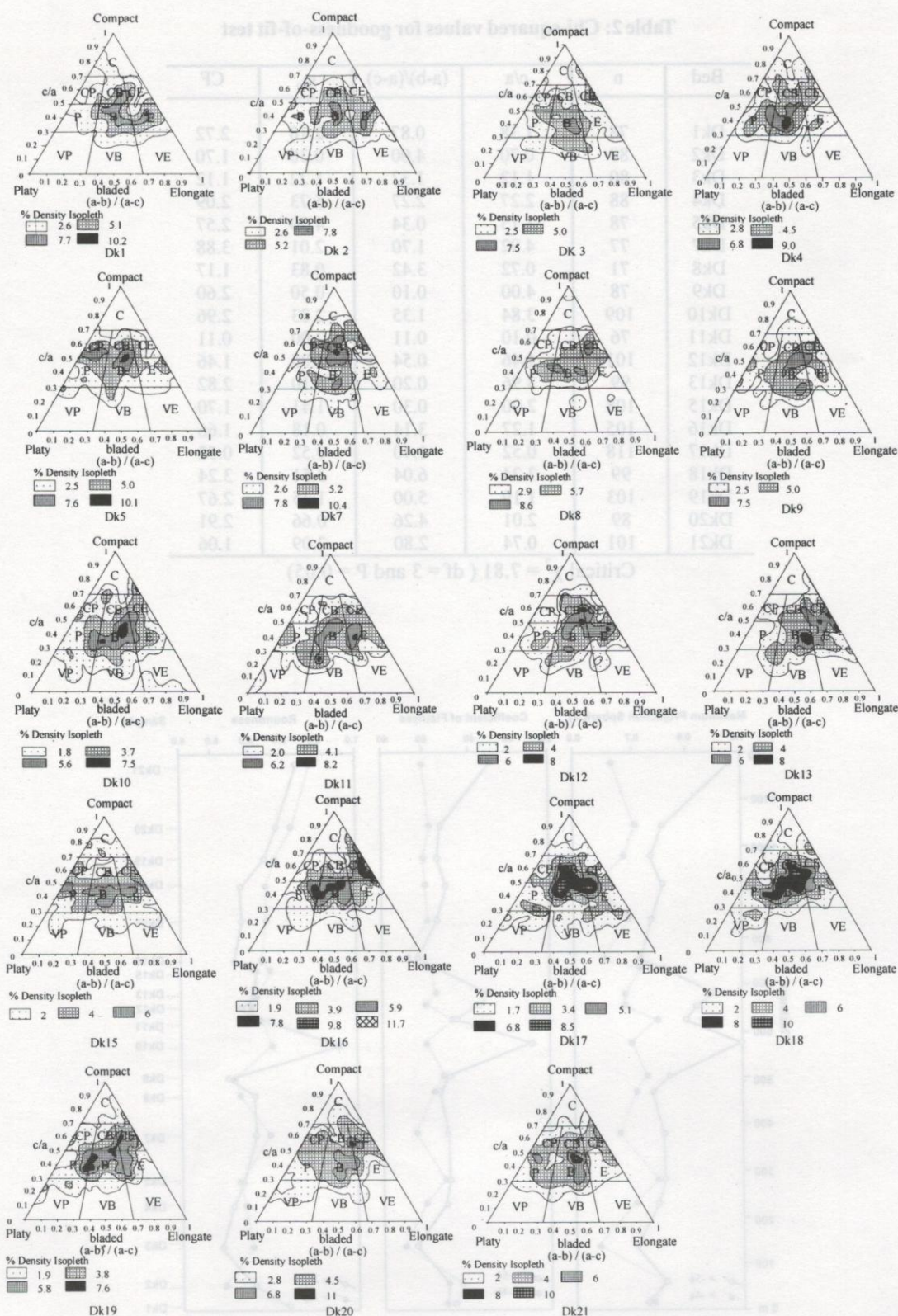


Fig. 4: Contoured shape diagrams of various clasts from conglomerates of the Dhan Khola Formation. Each diagram is divided into the following 10 fields, representing respectively compact (C), compact platy (CP), compact bladed (CB), compact elongate (CE), platy (P), bladed (B), elongate (E), very platy (VP), very bladed (VB), and very elongate (VE) forms.



Calculated t-values are listed in Table 4. The t-values obtained for axial ratios  $c/a$  and  $(a-b)/(a-c)$  are significant at levels between 0.10 and 0.01, but for other indices, the values obtained are insignificant. This implies that sampling means of  $\psi_p$ , CF, and  $\rho$  of quartzite and other clasts are similar although differences could exist for means of each sample.

Plots of mean axial ratios of quartzite and other clasts are shown in the shape diagrams (Fig. 5). The quartzite clasts belong to B (79%), CB (16%), and E (5%) whereas all other

clasts lie in the field of B. Therefore, the forms of the quartzite clasts do not deviate much from that of the other clasts. Generally, dolomite clasts tend to break along their laminae assuming flatter (low CF) forms. On the other hand, quartzite clasts are coarsely crystalline and tend to make more compact shapes. Modification of sphericity and axial ratios is slower in quartzite due to their competency. Hence, from the shape of quartzite clasts it can be inferred that they are not so matured.

**Table 3: Morphological indices of quartzite and other clasts in conglomerate from the Dhan Khola Formation, Surai Khola area**

Bed	Clast Type	n	c/a	(a-b)/(a-c)	$\psi_p$		CF		$\rho$	
					x	s	x	s	x	s
Dk1	Quartzite	54	0.44	0.59	0.66	0.09	44.0	10.5	3.00	1.11
	Other	24	0.42	0.61	0.64	0.12	41.8	4.7	3.04	0.51
Dk2	Quartzite	60	0.42	0.54	0.64	0.11	42.3	11.7	3.96	1.32
	Other	20	0.40	0.57	0.62	0.14	40.0	11.5	3.40	0.85
Dk3	Quartzite	16	0.53	0.58	0.73	0.11	53.2	13.7	4.31	1.22
	Other	64	0.40	0.56	0.62	0.12	39.8	15.3	4.75	0.64
Dk4	Quartzite	44	0.48	0.51	0.67	0.12	47.7	12.7	4.39	0.87
	Other	44	0.47	0.45	0.66	0.11	47.3	13.8	4.86	0.78
Dk5	Quartzite	29	0.45	0.46	0.64	0.11	44.7	11.2	4.33	0.80
	Other	49	0.44	0.47	0.65	0.10	44.5	19.0	4.29	0.81
Dk7	Quartzite	40	0.53	0.57	0.73	0.10	53.0	12.6	3.65	0.94
	Other	37	0.46	0.52	0.66	0.14	45.8	15.9	4.18	0.80
Dk8	Quartzite	60	0.47	0.57	0.69	0.10	47.3	10.0	4.30	1.12
	Other	11	0.42	0.53	0.63	0.15	42.1	17.0	4.96	0.52
Dk9	Quartzite	67	0.45	0.53	0.65	0.12	44.8	13.9	4.57	0.74
	Other	11	0.39	0.54	0.60	0.12	38.8	11.6	4.77	0.79
Dk10	Quartzite	19	0.45	0.55	0.66	0.13	45.4	14.7	3.16	1.49
	Other	90	0.41	0.51	0.62	0.13	40.9	13.4	3.19	1.24
Dk11	Quartzite	54	0.43	0.51	0.64	0.11	43.5	10.9	3.67	0.75
	Other	22	0.43	0.58	0.64	0.13	42.5	12.5	4.18	0.47
Dk12	Quartzite	33	0.48	0.57	0.69	0.11	47.9	12.4	4.14	0.55
	Other	68	0.41	0.55	0.63	0.13	41.0	13.0	3.45	0.95
Dk13	Quartzite	47	0.45	0.69	0.68	0.13	45.1	13.6	3.84	0.84
	Other	52	0.43	0.64	0.66	0.11	42.5	12.3	4.08	0.66
Dk15	Quartzite	57	0.47	0.58	0.69	0.13	49.1	17.6	3.59	1.00
	Other	51	0.42	0.44	0.62	0.11	41.9	0.13	3.64	0.92
Dk16	Quartzite	33	0.54	0.63	0.74	0.03	53.8	11.2	3.83	1.00
	Other	72	0.44	0.53	0.65	0.12	44.4	12.4	4.36	1.47
Dk17	Quartzite	54	0.48	0.56	0.69	0.09	47.5	11.8	3.81	0.94
	Other	64	0.43	0.46	0.63	0.13	42.9	13.5	3.41	1.12
Dk18	Quartzite	48	0.50	0.54	0.70	0.09	49.6	10.5	3.79	0.92
	Other	51	0.44	0.46	0.64	0.13	44.3	13.5	3.75	0.93
Dk19	Quartzite	42	0.50	0.59	0.70	0.10	49.8	12.1	3.40	1.07
	Other	61	0.42	0.48	0.63	0.14	42.5	13.8	3.99	1.01
Dk20	Quartzite	48	0.48	0.49	0.67	0.11	47.6	11.4	2.88	0.94
	Other	41	0.42	0.49	0.61	0.17	41.6	17.6	3.73	0.88
Dk21	Quartzite	48	0.48	0.50	0.68	0.13	48.1	13.4	2.60	0.66
	Other	53	0.40	0.50	0.61	0.13	40.9	12.8	3.08	0.81



**Table 4: Sampling means and standard deviations of morphological indices, and calculated t-values for the quartzite and other clasts in conglomerates**

	c/a	(a-b)/(a-c)	$\psi_p$	CF	$\rho$
Quartzite					
Mean	0.48	0.56	0.68	47.6	3.75
Standard deviation	0.12	0.05	0.11	12.4	1.04
Other					
Mean	0.42	0.52	0.63	42.4	3.95
Standard deviation	0.13	0.05	0.13	13.5	0.85
Calculated t values	1.73**	2.47***	1.28	1.24	0.65

\*\*P=0.05 and \*\*\*P=0.01

**Shape indices of different size-grades of quartzite clasts**

Shape indices of quartzite clasts (Table 5) are regarded as one of the reliable means of interpreting depositional environment, transport history and provenance of conglomerates. The degree of roundness depends on size, composition and history of transport (Pettijohn et al. 1987). Usually bigger clasts modify to higher values of indices with distance of transport and abrasion. Clasts with different size have different history of transport (Lindholm 1987 and Pettijohn 1984). Coarser clasts are better rounded than finer size grades (Lindholm 1987). But abnormal relation between two size grades and roundness may occur and is called 'textural inversion' (Folk 1980). In these, either angular coarse clasts and angular fine clasts or very angular and rounded clasts in same size-grade are expected to occur.

**Table 5: Morphological indices for different size-grades of quartzite clasts in conglomerates**

	Clast-Size mm	n	c/a	(a-b)/(a-c)	$\psi_p$		CF		$\rho$	
					x	s	x	s	x	s
Dk1	>-4 $\phi$	30	0.43	0.60	0.66	0.10	43.4	11.4	3.03	1.12
	>-5 $\phi$	23	0.45	0.58	0.67	0.09	44.9	9.54	2.98	1.12
Dk2	>-4 $\phi$	37	0.41	0.59	0.64	0.09	41.4	10.7	4.86	1.42
	>-5 $\phi$	20	0.45	0.44	0.64	0.13	44.6	13.1	4.00	1.10
Dk3	>-4 $\phi$	10	0.55	0.71	0.76	0.96	55.3	13.4	4.05	0.71
	>-5 $\phi$	5	0.52	0.36	0.69	0.11	52.3	15.0	4.90	0.89
Dk4	>-4 $\phi$	25	0.50	0.54	0.69	0.12	49.8	13.5	4.24	0.89
	>-5 $\phi$	19	0.45	0.49	0.65	0.11	44.8	11.4	4.57	0.81
Dk5	>-4 $\phi$	17	0.45	0.47	0.65	0.11	45.2	12.2	4.38	0.86
	>-5 $\phi$	12	0.44	0.45	0.64	0.11	44.1	10.8	4.25	0.75
Dk7	>-4 $\phi$	34	0.52	0.56	0.72	0.09	52.3	11.9	3.51	0.88
	>-5 $\phi$	5	0.45	0.45	0.64	0.13	44.8	15.0	3.90	1.14
Dk8	>-4 $\phi$	40	0.47	0.57	0.69	0.10	47.3	9.86	4.38	1.20
	>-5 $\phi$	15	0.46	0.46	0.66	0.09	46.5	9.31	3.97	1.18
Dk9	>-4 $\phi$	35	0.45	0.63	0.67	0.12	45.4	14.5	4.50	0.73
	>-5 $\phi$	32	0.44	0.43	0.63	0.12	44.1	13.4	4.66	0.77
Dk10	>-4 $\phi$	15	0.50	0.54	0.70	0.08	49.7	10.9	3.43	1.53
	>-5 $\phi$	2	0.25	0.75	0.50	0.20	24.7	15.5	1.50	0.00
Dk11	>-4 $\phi$	45	0.43	0.54	0.65	0.11	43.2	10.8	3.71	0.65
	>-5 $\phi$	7	0.42	0.30	0.60	0.10	42.5	10.7	3.50	1.15
Dk12	>-4 $\phi$	25	0.50	0.59	0.71	0.80	49.7	10.7	4.09	0.50
	>-5 $\phi$	6	0.37	0.46	0.58	0.15	37.1	13.4	4.33	0.75
Dk13	>-4 $\phi$	35	0.50	0.71	0.71	0.12	47.4	13.1	3.85	0.98
	>-5 $\phi$	8	0.30	0.47	0.55	0.16	34.8	14.3	3.94	0.74
Dk15	>-4 $\phi$	42	0.49	0.58	0.68	0.13	48.5	19.3	3.48	1.03
	>-5 $\phi$	8	0.48	0.30	0.64	0.09	47.5	12.1	3.88	0.52
Dk16	>-4 $\phi$	23	0.55	0.68	0.75	0.12	54.5	12.7	3.71	1.05
	>-5 $\phi$	6	0.52	0.33	0.68	0.34	51.6	4.73	4.50	0.83
Dk17	>-4 $\phi$	36	0.49	0.59	0.70	0.09	49.0	11.4	3.57	1.05
	>-5 $\phi$	15	0.47	0.47	0.66	0.09	46.6	10.9	4.30	1.37
Dk18	>-4 $\phi$	32	0.50	0.56	0.76	0.08	49.7	9.28	3.60	0.87
	>-5 $\phi$	11	0.45	0.45	0.64	0.11	44.8	11.5	4.32	0.98
Dk19	>-4 $\phi$	31	0.50	0.57	0.71	0.08	50.0	9.19	3.34	1.01
	>-5 $\phi$	8	0.47	0.55	0.66	0.15	46.9	19.5	3.63	1.24
Dk20	>-4 $\phi$	31	0.49	0.56	0.69	0.09	48.6	10.5	2.84	0.82
	>-5 $\phi$	17	0.46	0.38	0.64	0.13	45.9	12.9	3.27	0.87
Dk21	>-4 $\phi$	36	0.50	0.53	0.73	0.12	50.3	12.9	2.31	0.63
	>-5 $\phi$	7	0.35	0.22	0.52	0.09	34.6	7.10	2.71	0.76



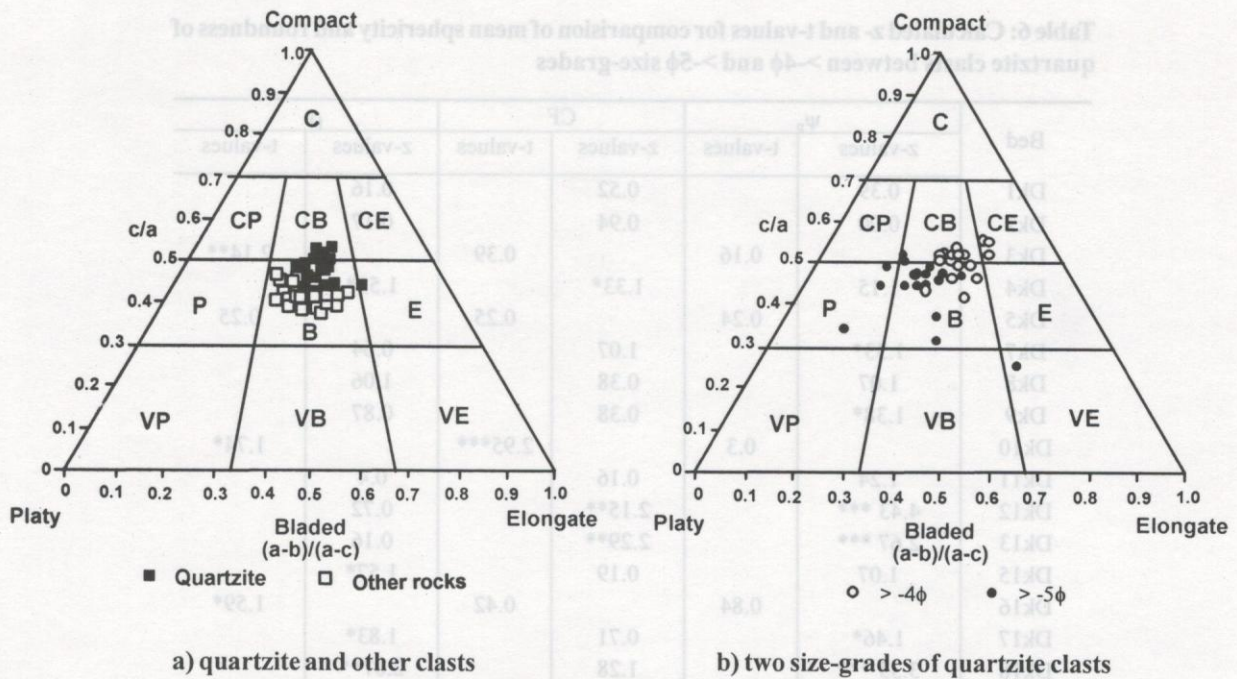


Fig. 5: Shape diagram of Sneed and Folk (1958) showing plots of mean axial ratios

To see any significant differences in means of  $\rho$ , and  $\psi_p$  for size-grades ( $>-4\phi$  and  $>-5\phi$ ), t- and z-values (Table 6) were calculated. Table 6 reveals that most (58%) of the samples (DK1, DK2, DK5, DK7, DK8, DK9, DK11, DK12, DK13, DK19, and DK21) have insignificant roundness values indicating textural inversion. Though the remaining 42% of samples show roundness values between the significance level of 0.1 and 0.05 (Table 6), they too (except DK10 and DK15) exhibit greater values of standard deviation (more than 0.65, see Table 5), and hence, textural abnormality.

The  $\psi_p$  for two size-grades of quartzite clasts are significantly different (0.1 to 0.01) for 42% of samples (Dk7, Dk9, Dk12, Dk13, Dk17, Dk18, Dk20, and Dk21, see Table 7).

Mean axial ratios of two size-grades of quartzite clasts were plotted on the shape-diagram (Fig. 5) of Sneed and Folk (1958). The diagram clearly separates plots of two size-grades. Smaller clasts plot on B, CB, and CE regions, whereas bigger do on VE, B, P, and CB regions of the diagram. It exhibits that smaller clasts have achieved somewhat higher maturity than that by bigger ones.

Means of CF considerably differ for 26% of the 19 samples at ranges of 0.10 to 0.01 significance levels (Table 6). Though a majority of samples do not show significant results, the shape diagram (Fig. 6c) clearly separates two size-grades of quartzite clasts.

**Sphericity versus coefficient of flatness**

The maximum projection sphericity,  $\psi_p$ , and CF are two useful indices used for discriminating clasts shaped in

different environments. Hence, these indices are palaeoenvironmental indicators giving clear figure in plot when quartzite clasts are considered (Howard 1992).

In Fig. 6a, b and c,  $\psi_p$  and CF correlate positively. Fig. 6a is the plot of average indices of all the clast types. It indicates that most of the samples do not plot on fluvial field. Fig. 6b shows that both indices for other clasts are lower than that for quartzite clasts. Consequently, the latter plots on the region beyond the lower index limits ( $\psi_p = 0.65$  and  $CF = 45$ , Stratten 1974). When different size-grades of quartzite clasts are considered only smaller size-grade plots on fluvial field (Fig. 6c) and the bigger does not. So, plots of Fig. 6b and 6c reveal differently.

**Comparison of shape indices with index limits**

Two shape indices ( $\psi_p$  and CF) of quartzite and other clasts (Table 3) were considered to compare with values of index limits proposed earlier (Stratten 1974). Dobkins and Folk (1970) and Gale (1990) have also proposed such limits for modern gravels. Table 7 lists results of comparison between shape indices and index limits. It shows that more than 60% of the indices of quartzite clasts are significantly greater than the lower limits. These clasts lie on the fluvial field of Fig. 6b and 6c, and clearly indicate that they were deposited in a fluvial environment. But it is also important to point out that, more than 95% of samples (with the significance level of 0.05) will be within the fluvial field if the limits of  $\psi_p$  and CF (Stratten 1974) were changed from 0.65 and 45 to 0.62 and 40, respectively for the Siwalik conglomerates.



**Table 6: Calculated z- and t-values for comparison of mean sphericity and roundness of quartzite clasts between  $>-4\phi$  and  $>-5\phi$  size-grades**

Bed	$\psi_p$		CF		$\rho$	
	z-values	t-values	z-values	t-values	z-values	t-values
Dk1	0.39		0.52		0.16	
Dk2	0.00		0.94		0.17	
Dk3		0.16		0.39		2.14**
Dk4	1.15		1.33*		1.52*	
Dk5		0.24		0.25		0.25
Dk7	1.33*		1.07		0.64	
Dk8	1.07		0.38		1.06	
Dk9	1.38*		0.38		0.87	
Dk10		0.3		2.95***		1.74*
Dk11	1.24		0.16		0.4	
Dk12	4.43 ***		2.15**		0.72	
Dk13	2.67 ***		2.29**		0.16	
Dk15	1.07		0.19		1.57*	
Dk16		0.84		0.42		1.59*
Dk17	1.46*		0.71		1.83*	
Dk18	3.33 ***		1.28		2.07**	
Dk19	0.91		0.44		0.61	
Dk20	1.41*		0.74		3.04**	
Dk21	5.39 ***		4.59***		0.72	

\*P=0.1, \*\*P=0.05 and \*\*\*P=0.01

**Table 7: Obtained t-values for  $\psi_p$  and CF after comparing with the limits ( $\psi_p=0.65$  and CF=45) of Stratten (1974)**

Bed	Quartzite clasts		Other clasts	
	$\psi_p$	CF	$\psi_p$	CF
Dk1	0.82	-0.70	-0.41	-3.36
Dk2	-0.70	-1.79	-0.96	-1.94
Dk3	2.91***	2.39***	-2.00	-2.72
Dk4	1.11	1.41*	0.60	1.11
Dk5	-0.49	0.14	0.00	-0.18
Dk7	5.06***	4.06***	0.43	0.31
Dk8	3.10***	1.78**	0.44	-0.57
Dk9	0.00	-0.12	-1.38	-1.77
Dk10	0.34	0.12	-2.19	-2.90
Dk11	0.67	-1.01	-0.36	-0.94
Dk12	2.09**	1.34*	-1.27	-2.54
Dk13	1.99**	0.05	0.66	-1.47
Dk15	2.32**	1.76**	-1.95	-1.70
Dk16	17.0***	4.51***	0.00	-0.41
Dk17	4.08***	1.56*	-1.23	-1.24
Dk18	3.85***	3.04***	-0.55	-0.37
Dk19	3.24***	2.57***	-1.12	-1.42
Dk20	1.26*	1.58*	-1.51	-1.24
Dk21	1.60*	1.60*	-2.24	-2.33

\* P=0.1 \*\*P=0.05 and \*\*\*P=0.01



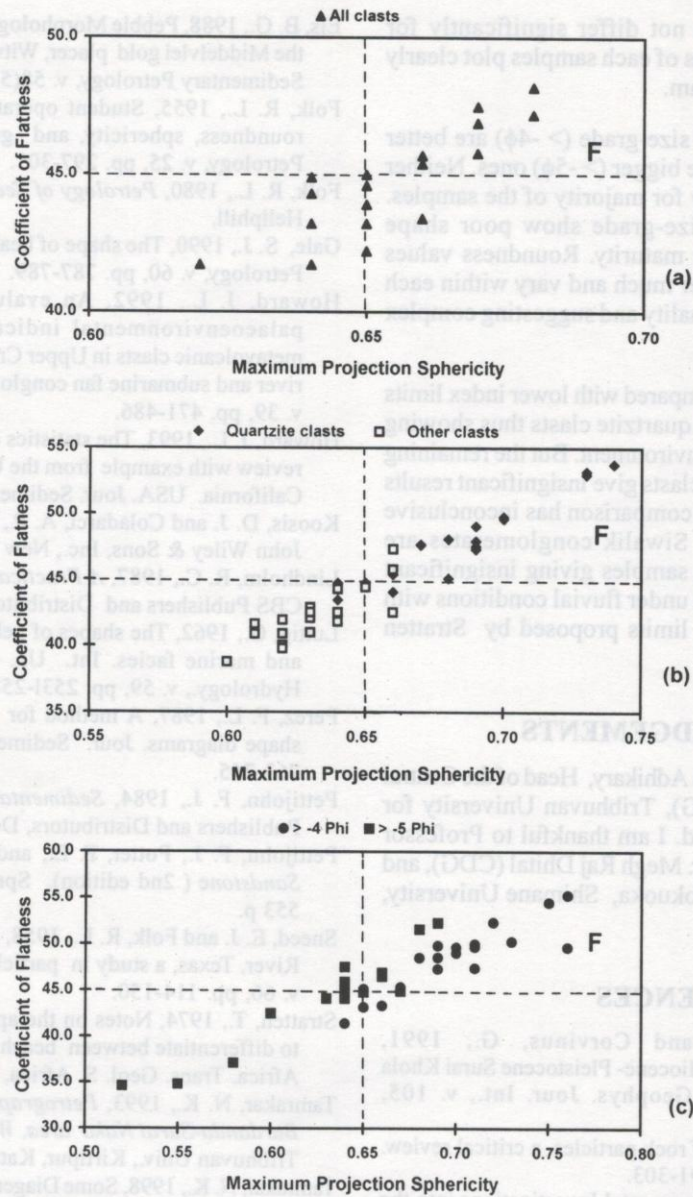


Fig. 6: Plots of maximum projection sphericity versus coefficient of flatness for (a) each sample, (b) quartzite and other clasts, and (c) different size-grades of quartzite clasts. Dashed lines in diagrams represent lower index limits of Stratten (1974) for pebbles shaped in fluvial environment (F).

### CONCLUSIONS

On the basis of dominance of clast-type, the Dhan Khola Formation can be divided into the volcanic clast-dominated unit, dolomite clast-dominated unit, quartzite clast-dominated unit, and the terrigenous clast-dominated unit from the lower to the upper part, respectively. The change in distribution of clasts from metamorphic source (quartzite and dolomite) to sedimentary source (terrigenous rocks), and appearance of clasts of the Siwalik rocks in the middle part of the formation is attributed to a gradual unroofing of the Siwaliks in the north.

Trends of variation of  $\psi_p$ , CF, and  $\rho$  of bigger size-grade of the quartzite clasts are more-or-less similar in the vertical sequence. The bigger clasts are better rounded in the younger unit. The roundness values of both bigger and smaller size-grades decrease simultaneously towards the upper unit indicating nearness of province or rapid transport of those clasts during deposition of the younger unit.

On the shape diagram of Sneed and Folk (1958), quartzite clasts tend to plot on CB field, whereas other clasts on B field. This difference may be related to their inherent properties and history of transport.



Although  $\psi_p$  and CF do not differ significantly for quartzite and other clast, means of each samples plot clearly on sphericity versus CF diagram.

Quartzite clasts of smaller size-grade ( $> -4\phi$ ) are better sphered with higher  $\psi_p$  than the bigger ( $> -5\phi$ ) ones. Neither  $\psi_p$  nor CF differs significantly for majority of the samples. Quartzite clasts of bigger size-grade show poor shape modification indicating lower maturity. Roundness values of two size-grades do not differ much and vary within each grade showing textural abnormality and suggesting complex source of these clasts.

The means of  $\psi_p$  and CF compared with lower index limits are significant for 60% of the quartzite clasts thus showing that they are shaped in fluvial environment. But the remaining samples of quartzite and other clasts give insignificant results probably suggesting that such comparison has inconclusive result when clasts from the Siwalik conglomerates are considered. Alternatively, the samples giving insignificant results could have also formed under fluvial conditions with  $\psi_p$  and CF limits lower than limits proposed by Stratten (1974).

#### ACKNOWLEDGEMENTS

I thank Dr. Prakash Chandra Adhikary, Head of the Central Department of Geology (CDG), Tribhuvan University for support and facilities provided. I am thankful to Professor Madhav Prasad Sharma and Dr. Megh Raj Dhital (CDG), and professors S. Yokota and T. Tokuoka, Shimane University, Japan for their suggestions.

#### REFERENCES

- Appel, E., Rostler, W., and Corvinus, G., 1991, Magnetostratigraphy of the Miocene- Pleistocene Surai Khola Siwaliks in West Nepal. *Geophys. Jour. Int.*, v. 105, pp. 191-198.
- Barrett, P. J., 1980, The shape of rock particles, a critical review. *Sedimentology*, v. 27, pp. 291-303.
- Corvinus, G., 1992, Palaeoenvironmental Investigations into the Siwaliks in Nepal (The Litho- and biostratigraphy of Surai Khola, Western Nepal). *Bull. Dept. Geology*, v. 2(1), pp. 75-87.
- Dhital, M. R., Gajurel, A. P., Pathak, D., Paudel, L.P., and Kizaki, K., 1995, Geology of Mid Western Nepal Around the Rapti River. *Bull. Dept. Geology*, v. 4, Sp. Issue, pp. 1-70.
- Dobkins, J. E. and Folk, R. L., 1970, Shape development on Tahiti-Nui. *Jour. Sedimentary Petrology*, v. 40, pp. 1167-1203.
- Els, B. G., 1988, Pebble Morphology of an ancient conglomerate: the Middelvllei gold placer, Witwatersrand, South Africa. *Jour. Sedimentary Petrology*, v. 58(5), pp. 894-901.
- Folk, R. L., 1955, Student operator error in determination of roundness, sphericity, and grain size. *Jour. Sedimentary Petrology*, v. 25, pp. 297-301.
- Folk, R. L., 1980, *Petrology of Sedimentary Rock*. Austin, Tex., Hellphill.
- Gale, S. J., 1990, The shape of beach pebbles. *Jour. Sedimentary Petrology*, v. 60, pp. 787-789.
- Howard, J. L., 1992, An evaluation of shape indices as palaeoenvironmental indicators using quartzite and metavolcanic clasts in Upper Cretaceous to Palaeogene beach, river and submarine fan conglomerates. *Jour. Sedimentology*, v. 39, pp. 471-486.
- Howard, J. L., 1993, The statistics of counting clasts in rudites: a review with example from the Upper Palaeogene of Southern California. *USA. Jour. Sedimentology*, v. 40, pp. 157-174.
- Koosis, D. J. and Coladarci, A. P., 1985, *Statistics* (3rd edition). John Wiley & Sons, Inc., New York, 286 p.
- Lindholm, R. C., 1987, *A Practical approach to Sedimentology*. CBS Publishers and Distributors, Delhi, 276 p.
- Luttig, G., 1962, The shapes of pebbles in continental, fluvial and marine facies. *Int. Un. Geol. Geophysics, Ass. Sci. Hydrology.*, v. 59, pp. 2531-258.
- Perez, F. L., 1987, A method for contouring triangular particle shape diagrams. *Jour. Sedimentary Petrology*, v. 57(4), pp. 763-765.
- Pettijohn, F. J., 1984, *Sedimentary Rocks* (3rd edition). CBS Publishers and Distributors, Delhi, 628 p.
- Pettijohn, F. J., Potter, P. E., and Siever, R., 1987, *Sand and Sandstone* (2nd edition). Springer Verlag New York Inc., 553 p.
- Sneed, E. J. and Folk, R. L., 1958, Pebbles in the lower Colorado River, Texas, a study in particle morphogenesis. *Jour. Geol.*, v. 66, pp. 114-150.
- Stratten, T., 1974, Notes on the application of shape parameters to differentiate between beach and river deposits in southern Africa. *Trans. Geol. S. Africa*, v. 77, pp. 59-64.
- Tamrakar, N. K., 1993, *Petrography of the Siwalik rocks of the Bardanda-Surai Naka area, West Nepal*. M. Sc. thesis of the Tribhuvan Univ., Kirtipur, Kathmandu, 139 p (unpublished).
- Tamrakar, N. K., 1998, Some Diagenetic Characteristics of Arenites From the Siwaliks, Surai Khola Area, Mid Western Nepal. *Bull. Dept. Geol.*, v. 6, pp. 89-98.
- Tokuoka, T., Takayasu, K., Yoshida, M., and Hisatomi, K., 1986, The Churia (Siwalik) Group of the Arung Khola Area, West Central Nepal. *Mem, Fac. Sci., Shimane Univ.*, v. 20, pp. 135-210.
- Tokuoka, T., 1992, The Churia (Siwalik) Group in West Central Nepal. *Bull. Dept. Geology*, v. 2(1), pp. 75-87.